Selective tumor antigen vaccine delivery to human CD169$^+$ antigen-presenting cells using ganglioside-liposomes

Alsya J. Affandi[a], Joanna Grabowska[a], Katarzyna Olesek[a], Miguel Lopez Venegas[a,b], Arnaud Barbaria[a], Ernesto Rodríguez[a], Patrick P. G. Mulder[a], Helen J. Pijffers[a], Martino Ambrosini[a], Hakan Kalay[a], Tom O'Toole[a], Eline S. Zwart[a,c], Geert Kazemier[c], Kamran Nazmi[d], Floris J. Bikker[d], Johannes Stöckl[e], Alfons J. M. van den Eertwegh[f], Tanja D. de Gruijl[f], Gert Storm[g,h], Yvette van Kooyk[a,b], and Joke M. M. den Haan[a,1]

[a]Department of Molecular Cell Biology and Immunology, Cancer Center Amsterdam, Amsterdam Infection and Immunity Institute, Amsterdam UMC, Vrije Universiteit Amsterdam, 1081 HZ Amsterdam, The Netherlands; [b]DC4U, 3621 ZA Breukelen, The Netherlands; [c]Department of Surgery, Cancer Center Amsterdam, Amsterdam UMC, Vrije Universiteit Amsterdam, 1081 HV Amsterdam, The Netherlands; [d]Department of Oral Biochemistry, Academic Centre for Dentistry Amsterdam (ACTA), Vrije Universiteit Amsterdam and University of Amsterdam, 1081 LA Amsterdam, The Netherlands; [e]Institute of Immunology, Centre for Pathophysiology, Infectiology and Immunology, Medical University of Vienna, 1090 Vienna, Austria; [f]Department of Medical Oncology, Cancer Center Amsterdam, Amsterdam UMC, Vrije Universiteit Amsterdam, 1081 HV Amsterdam, The Netherlands; [g]Department of Pharmaceutics, Utrecht Institute for Pharmaceutical Sciences, Utrecht University, 3508 TB Utrecht, The Netherlands; and [h]Department of Biomaterials, Science and Technology, Faculty of Science and Technology, University of Twente, 7522 NB Enschede, The Netherlands

Edited by Peter Cresswell, Yale University, New Haven, CT, and approved September 3, 2020 (received for review April 2, 2020)

Priming of CD8$^+$ T cells by dendritic cells (DCs) is crucial for the generation of effective antitumor immune responses. Here, we describe a liposomal vaccine carrier that delivers tumor antigens to human CD169/Siglec-1$^+$ antigen-presenting cells using gangliosides as targeting ligands. Ganglioside-liposomes specifically bound to CD169 and were internalized by in vitro-generated monocyte-derived DCs (moDCs) and macrophages and by ex vivo-isolated splenic macrophages in a CD169-dependent manner. In blood, high-dimensional reduction analysis revealed that ganglioside-liposomes specifically targeted CD14$^+$ CD169$^+$ monocytes and Axl$^+$ CD169$^+$ DCs. Liposomal codelivery of tumor antigen and Toll-like receptor ligand to CD169$^+$ moDCs and Axl$^+$ CD169$^+$ DCs led to cytokine production and robust cross-presentation and activation of tumor antigen-specific CD8$^+$ T cells. Finally, Axl$^+$ CD169$^+$ DCs were present in cancer patients and efficiently captured ganglioside-liposomes. Our findings demonstrate a nanovaccine platform targeting CD169$^+$ DCs to drive antitumor T cell responses.

Siglec-1 | CD169 | dendritic cells | CD8$^+$ T cells | vaccination

The major breakthrough of immune-checkpoint inhibitors, such as anti-CTLA4 and anti–PD-L1, in cancer therapy is still limited to a minority of patients who respond to this treatment (1). Patients with pancreatic cancer, for example, failed to respond to monotherapies of checkpoint inhibitors in multiple trials (2, 3). Factors such as poor tumor immunogenicity, tumor-immunosuppressive microenvironment, and the lack of an existing tumor-specific immune response are thought to contribute to patients' lack of response to these immune-checkpoint inhibitors (2, 4, 5). Nevertheless, the abundance of intratumoral CD8$^+$ T cells is associated with longer survival of pancreatic cancer patients, suggesting these patients may benefit from a better antitumor immunity (6–8). Therefore, new strategies aiming to boost patients' antitumor CD8$^+$ T cell responses should be explored to improve current therapies.

Dendritic cells (DCs) play a crucial role in eliciting immune responses against tumor-specific antigens and have therefore generated significant interest as a therapeutic target in the context of cancer immunotherapy (9). The most commonly used DC-based immunotherapy utilizes monocyte-derived DCs (moDCs) due to the large numbers that can be generated ex vivo. In general, moDC-based vaccines have shown some survival benefit and appear to be well-tolerated; however, the objective response rate in most studies is still relatively low (9, 10). Moreover, since generating DCs ex vivo is a laborious, time-consuming, and costly process, research is shifting toward targeting tumor antigens to naturally circulating or tissue-resident DCs in vivo as a vaccine strategy to induce immune responses (11). Both in mice and humans, DCs can be divided into several subsets, of which the conventional DCs (CD141$^+$ cDC1 and CD1c$^+$ cDC2) have been shown to be responsible for T cell priming (12, 13).

In vivo DC targeting can be achieved by using antibodies or ligands that bind to DC-specific receptors and are directly conjugated to tumor antigen or to nanoparticles harboring tumor antigen. Targeting C-type lectin receptors in particular, such as DEC-205, Clec-9A, and DC-SIGN, has been demonstrated to induce antigen-specific and antitumor responses in mouse and human models (14–17). Recently, we compared two vaccination

Significance

Current immunotherapies only benefit a minority of all cancer patients, so it is necessary to develop other strategies to boost patients' antitumor CD8$^+$ T cell responses. Here, we formulated a liposomal vaccine carrier that selectively delivers tumor antigens and Toll-like receptor agonists to human CD169/Siglec-1$^+$ antigen-presenting cells (APCs) through the incorporation of gangliosides that are natural ligands of CD169. This liposomal vaccine binds to a variety of human CD169$^+$ APCs, including monocyte-derived dendritic cells (moDCs) and the recently described Axl$^+$ DCs. Uptake of the vaccine results in robust cross-presentation and activation of tumor antigen-specific CD8$^+$ T cells. Our findings demonstrate a unique vaccination platform by targeting human CD169$^+$ DCs to stimulate antitumor T cell responses.

Author contributions: A.J.A. and J.M.M.d.H. designed research; A.J.A., J.G., K.O., M.L.V., A.B., E.R., P.P.G.M., H.J.P., M.A., H.K., T.O., K.N., and F.J.B. performed research; K.N., F.J.B., and J.S. contributed new reagents/analytic tools; A.J.A., J.G., and K.O. analyzed data; A.J.A., J.G., E.R., M.A., T.O., E.S.Z., G.K., J.S., A.J.M.v.d.E., T.D.d.G., G.S., Y.v.K., and J.M.M.d.H. wrote the paper; E.S.Z., G.K., A.J.M.v.d.E., and T.D.d.G. provided patient materials and information; and T.D.d.G., Y.v.K., and J.M.M.d.H. supervised the study.

The authors declare no competing interest.

This article is a PNAS Direct Submission.

[1]To whom correspondence may be addressed. Email: j.denhaan@amsterdamumc.nl.

This article contains supporting information online at https://www.pnas.org/lookup/suppl/doi:10.1073/pnas.2006186117/-/DCSupplemental.

First published October 16, 2020.

strategies of antigen–antibody conjugates directed to either DEC-205$^+$ DCs or to CD169$^+$ macrophages, a type of macrophage that acts as sentinel in secondary lymphoid organs (18). Remarkably, we observed that antigen targeting toward CD169$^+$ macrophages led to a significant antigen-specific CD8$^+$ T cell response that was as efficient as DEC-205 targeting and capable of suppressing tumor cell outgrowth (18–20). Stimulation of antigen-specific immune responses by targeting to CD169 has also been demonstrated using HLA-A2.1 transgenic mice and human CD169-expressing moDCs (21), indicating the immunotherapy potential of antigen targeting to CD169.

In a resting state, CD169/Siglec-1 is highly expressed by a specific subtype of macrophages that are located bordering the marginal zone in the spleen and the subcapsular sinus of lymph nodes (22, 23). Their strategic location allows them to be among the first cells to encounter and to capture blood and lymph-borne pathogens, and, in conjunction with DCs, to initiate the appropriate immune responses (18, 19, 24, 25). In addition to combating infection, CD169$^+$ macrophages have been implicated in antitumor immunity. They have been shown to capture tumor-derived materials in mouse and human (26, 27), and their frequency in tumor-draining lymph nodes is clearly associated with better clinical outcomes in several types of cancer (28–30). Although the exact mechanism is unclear, these observations suggest that lymphoid-resident CD169$^+$ macrophages can positively contribute to antitumor immunity. Next to lymphoid tissue-resident macrophages, CD169 is also constitutively expressed by a recently described Axl$^+$ Siglec6$^+$ DC subset (Axl$^+$ DCs, AS DCs, or pre-DCs) present in peripheral blood and lymphoid tissues (31–34). Axl$^+$ DCs have been proposed as a distinct DC subset that has the capacity to produce inflammatory cytokines and to stimulate CD4$^+$ and CD8$^+$ T cells (31–33). In addition to these constitutively CD169-expressing macrophages and DCs, during inflammatory conditions, monocytes can up-regulate CD169 in response to type I interferons (IFN-Is) (35, 36).

CD169 is a member of the sialic acid-binding Ig-like lectin (Siglec) receptor family that recognizes sialic acids present on glycoproteins or glycolipids on the cell surface and mediates cell–cell interactions and adhesion (37). Sialic acid-containing glycosphingolipids, such as GM3, GT1b, and GD1a gangliosides, are known to be endogenous ligands for CD169 molecules (38, 39). However, the CD169–sialic acid axis can be hijacked as a receptor entry molecule by viral pathogens, including murine leukemia virus (MLV), HIV, and Ebola virus to infect DCs or macrophages (40–43). The CD169-mediated entry and transinfection is dependent on gangliosides, including GM3, that are present on the viral lipid membrane (40, 44, 45). Interestingly, Axl$^+$ DCs have been recently demonstrated to be the predominant DC subset to capture HIV in a CD169-dependent manner.

In this study, we aimed to exploit ganglioside–CD169 interactions to develop a novel tumor antigen vaccination strategy that directs tumor antigens to human CD169$^+$ antigen-presenting cells (APCs) using liposomes containing gangliosides. We generated liposomes with different types of gangliosides and assessed the binding and uptake by different types of human CD169$^+$ APCs, including monocytes and primary and monocyte-derived macrophages and DCs. High-dimensionality mapping revealed the specificity of ganglioside-liposome targeting exclusively to circulating CD169$^+$ monocytes and Axl$^+$ DCs. To determine the efficacy of ganglioside-liposomes for antigen presentation, we encapsulated peptides derived from the pancreatic cancer-associated tumor antigen Wilms tumor 1 (WT1) or melanoma-associated gp100 antigen into the ganglioside-liposomes. CD169$^+$ moDCs and Axl$^+$ DCs loaded with these ganglioside-liposomes efficiently activated CD8$^+$ T cells specific for these epitopes. Moreover, Axl$^+$ DCs were present in patients with four different cancers and could be targeted by ganglioside-liposomes. Our data demonstrate that ganglioside-liposomes can be used as nanovaccine carriers that efficiently target CD169$^+$ DCs for cross-presentation and antigen-specific T cell activation. In conclusion, our studies support the concept that cancer vaccines targeting to CD169 can be applied to boost CD8$^+$ T cell responses in cancer patients.

Results

Ganglioside-Liposomes Bind to Recombinant Human CD169 and CD169-Overexpressing THP1 Cells. To generate nanovaccines targeting CD169, we formulated five different EPC/EPG/cholesterol-based liposomes, each containing 3% of one of five gangliosides, GM3, GD3, GM1, GT1b, or GD1a (Fig. 1*A* and *SI Appendix*, Table S1 and Fig. S1), with a diameter of ∼200 nm and negatively charged. These gangliosides are known to bind to CD169 with different affinities (39, 46). To assess binding to CD169, we performed an ELISA-based assay in which the binding of human recombinant CD169 to plate-bound liposomes was tested. We observed significant binding of all ganglioside-liposomes to CD169, and GD1a-liposome was the strongest binder (Fig. 1*B*). In contrast, control liposomes, with no ganglioside incorporated, did not bind to recombinant CD169.

We incorporated lipophilic fluorescent tracer DiD into the ganglioside-liposomes to evaluate the binding and uptake by CD169-overexpressing cells (*SI Appendix*, Fig. S1). Using the human monocytic cell line THP-1 overexpressing CD169 (TSn), we determined the cellular binding of ganglioside-liposomes at 4 °C. We observed that, while all ganglioside-liposomes showed clear binding to TSn cells, GD1a- and GT1b-liposomes showed the most binding (Fig. 1 *C* and *D*). All ganglioside-liposomes were taken up in a dose-dependent manner at 37 °C (Fig. 1*E*). Ganglioside-liposome binding and uptake was CD169-dependent, as it was absent in CD169-negative THP-1 cells (*SI Appendix*, Fig. S1), and preincubation with anti-CD169 antibody (clone 7–239) prevented binding and uptake of ganglioside-liposomes by TSn (Fig. 1 *F* and *G*). Collectively, these results indicate that ganglioside-liposomes specifically bind to CD169 and CD169-overexpressing TSn cells.

Ganglioside-Liposomes Target Human Monocyte-Derived Macrophages and Primary Splenic Macrophages. We have previously demonstrated an efficient vaccination strategy by antigen targeting to CD169$^+$ macrophages using antibodies in mouse models (18, 19). To determine whether ganglioside-liposomes could potentially target antigens to human CD169$^+$ macrophages, we tested the expression of CD169 on human monocyte-derived macrophages (moMacs). CD169 was already highly expressed by moMacs, and this expression was further elevated by IFNα treatment (*SI Appendix*, Fig. S2). Similar to TSn, moMacs bound and internalized ganglioside-liposomes in a CD169-dependent manner (Fig. 2 *A*–*C*). Addition of IFNα further boosted binding and uptake of ganglioside-liposome by moMacs (*SI Appendix*, Fig. S2).

To determine whether human primary macrophages can bind and take up ganglioside-containing liposomes, a liposome uptake assay was performed with human splenocytes. Human splenic red pulp macrophages were defined by high autofluorescence and expression of HLA-DR and CD163 and were found to also express CD169 (Fig. 2 *D* and *E*) (47). Upon addition of ganglioside-liposomes, the primary macrophages took up ganglioside-liposomes, and this process was mediated by CD169 (Fig. 2 *F* and *G*). This indicates that ganglioside-incorporated liposomes are able to target both human in vitro-derived and ex vivo primary splenic macrophages.

Ganglioside-Liposomes Are Bound and Internalized by Human moDCs in a CD169-Dependent Manner. Human moDCs express low levels of CD169 that can be up-regulated by addition of IFNα to the culture; thus, we next determined whether ganglioside-liposomes could target CD169$^+$ moDCs. Indeed, treatment of moDCs with

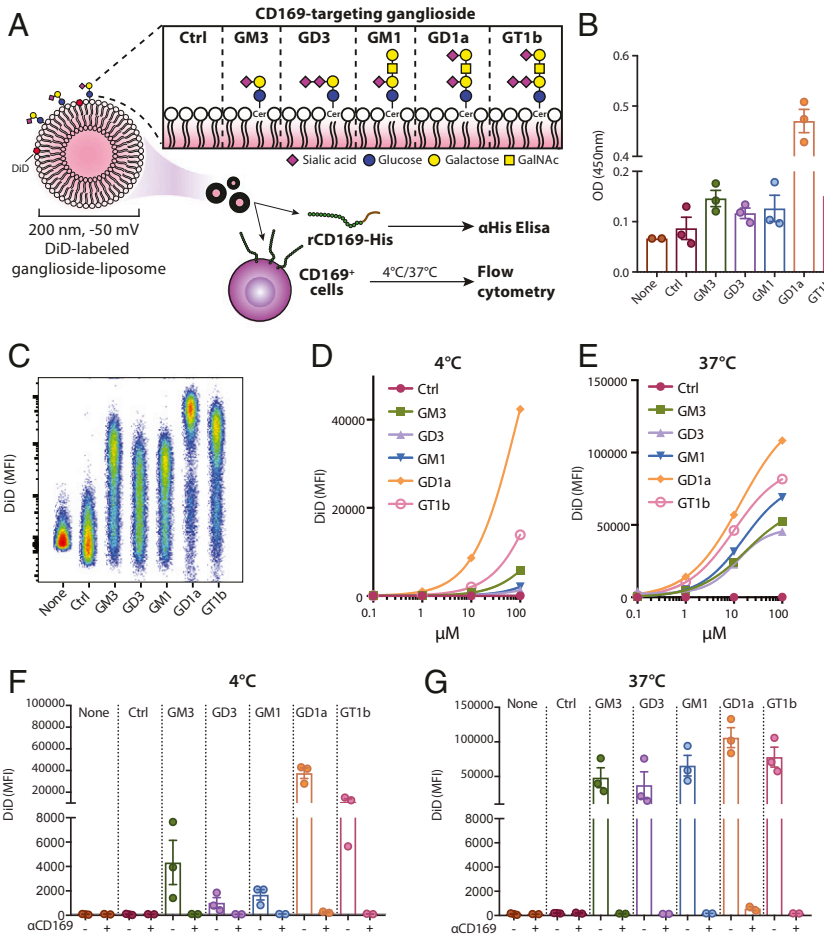

Fig. 1. Ganglioside-liposomes bind CD169 and CD169-overexpressing THP-1. (*A*) Gangliosides GM3, GD3, GM1, GD1a, and GT1b were incorporated into liposomes, and binding to CD169 was determined by recombinant CD169 ELISA or cell-based flow cytometry. GalNAc, N-acetyl galactosamine; Cer, ceramide; Ctrl, control. (*B*) Binding of recombinant human CD169 (rCD169) to ganglioside-liposomes as determined by ELISA. (*C*–*G*) DiD-labeled ganglioside-liposomes were incubated with THP-1 cells overexpressing CD169 (TSn), and binding at 4 °C or uptake at 37 °C was determined by flow cytometry. (*C*) Representative plot of ganglioside-liposome binding (100 μM) to TSn. (*D* and *E*) Binding or uptake of ganglioside-liposomes at different concentrations from one representative experiment out of two is shown. (*F* and *G*) TSn were preincubated with anti-CD169 blocking antibody at 4 °C for 15 min to show specificity of 100 μM ganglioside-liposome binding or uptake. Data are mean ± SEM from three independent experiments.

IFNα increased the expression of CD169 on moDCs and resulted in enhanced ganglioside-liposome binding and uptake (*SI Appendix*, Fig. S2). The binding and uptake of ganglioside-containing liposomes by moDCs was blocked by anti-CD169 antibody (Fig. 3 *B* and *C*). This indicates that the binding and uptake of ganglioside-liposomes on moDCs was exclusively mediated by CD169 despite the expression of other Siglecs by moDCs (48). Furthermore, using imaging flow cytometry, we confirmed the internalization of ganglioside-liposomes within 1 to 2 h (Fig. 3 *D* and *E*). All ganglioside-liposomes were internalized efficiently by moDCs without noticeable differences. Thus, ganglioside-liposomes specifically bind to and are internalized by CD169-expressing moDCs.

Ganglioside-Liposomes Harboring Toll-Like Receptor Ligand Activate CD169$^+$ moDCs and Are Cross-Presented to T Cells. To determine whether ganglioside-liposomes could be used as a nanovaccine to target tumor antigen and adjuvant to CD169$^+$ APCs, we used CD169$^+$ moDCs and formulated ganglioside-liposomes containing Toll-like receptor (TLR) 4 ligand MPLA and tumor-associated WT1 antigen (Fig. 4*A*). MPLA-containing liposomes have been previously shown to activate moDCs, and its incorporation did not interfere with ganglioside-liposome binding to moDCs (*SI Appendix*, Fig. S3) (49). Uptake of MPLA-containing ganglioside-liposomes stimulated IL-6 production by the moDCs, which indicates specific activation of the moDCs (Fig. 4*B*). To assess antigen presentation, we incubated moDCs with ganglioside-liposomes containing MPLA and WT1 peptide for 45 min, washed the cells, and cocultured them with WT1-specific CD8$^+$ T cells for 16 to 24 h. moDCs loaded with ganglioside/WT1/MPLA-liposomes, but not control liposomes, stimulated IFNγ secretion by CD8$^+$ T cells (Fig. 4 *C* and *D*). Interestingly, all ganglioside-liposomes were able to induce similar levels of IFNγ despite differences in binding and uptake to moDCs.

Second, we assessed the capacity of ganglioside-liposomes to stimulate cross-presentation using melanoma-associated gp100 antigen. For these studies, we used GM3-containing liposomes, as GM3 has been shown to be the ganglioside responsible for binding of multiple viruses to CD169 (40). We incorporated gp100 long peptide into GM3-liposomes, and, as an additional comparison, we used DC-SIGN-targeting Lewis Y-containing liposomes, for which cross-presentation was previously demonstrated (50). After uptake of gp100-containing liposomes, we cocultured moDCs with gp100-specific T cells and assessed IFNγ secretion. We observed that GM3/gp100-liposomes induced IFNγ secretion by the gp100-specific T cells, and the level was

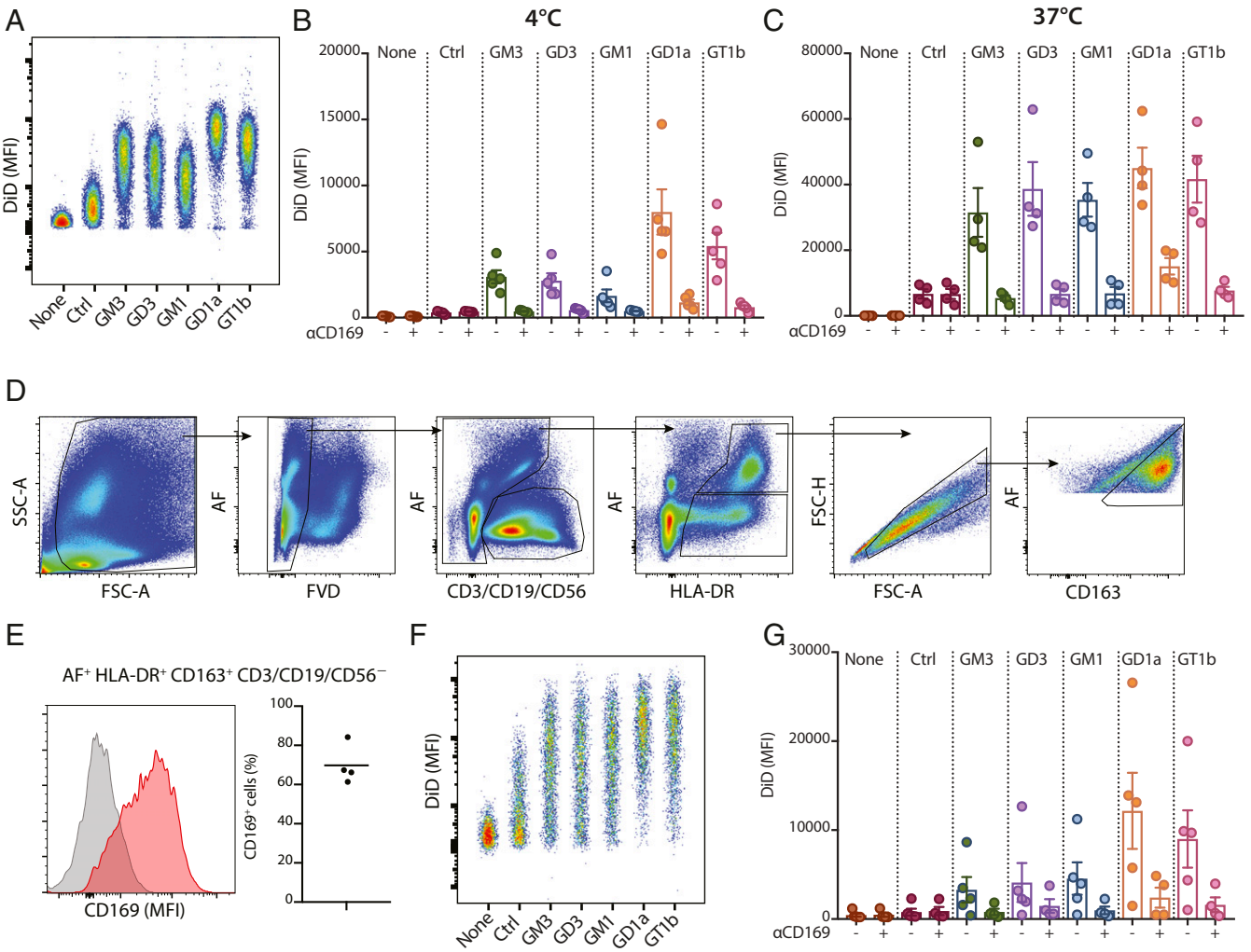

Fig. 2. Ganglioside-liposomes bind CD169-expressing moMacs and human splenic macrophages. (*A* and *B*) DiD-labeled ganglioside-liposomes were incubated with moMacs, and binding (4 °C; *A* and *B*) and uptake (37 °C; *C*) was determined by flow cytometry. Data are mean ± SEM from four independent donors. (*D*) Human spleen cells were incubated with ganglioside-liposomes at 37 °C for 45 min and stained for cell lineage markers. Gating strategy of autofluorescence$^+$ (AF) HLA-DR$^+$ CD163$^+$ CD3/CD19/CD56$^-$ macrophages is displayed. (*E*) The expression of CD169 on human splenic macrophages is shown as a representative histogram (*Left*; gray, fluorescence minus one; red, CD169) and percentages (*Right*; $n = 4$). (*F* and *G*) Ganglioside-liposome uptake by human splenic macrophages as (*F*) representative dot plot and (*G*) quantification ($n = 4$ to 5) is shown. When indicated, macrophages were preincubated with anti-CD169 blocking antibody to block ganglioside-liposome binding. Data are mean ± SEM from $n = 4$ to 5 donors.

comparable to Lewis Y-liposomes (Fig. 4 *E* and *F*). This indicates that ganglioside-liposome can be used to deliver antigen for cross-presentation to T cells.

Ganglioside-Liposomes Target Primary Human CD14$^+$ CD169$^+$ Monocytes and Axl$^+$ DCs. CD169-expressing immune cells can be identified in blood, and their frequency is increased under various inflammatory conditions (35, 36). To investigate which circulating immune cells can bind ganglioside-liposomes, we isolated PBMCs from healthy donors and assessed liposome uptake ex vivo. We performed unsupervised high-dimensionality reduction viSNE analysis of HLA-DR$^+$ CD3/CD19/CD56$^-$ APCs using the monocyte and DC lineage markers CD14, CD16, CD123, CD11c, CD1c, CD141, Axl, Siglec-6, and CD169 (Fig. 5*A*). We were able to identify distinct populations of monocytes, including classical (CD14$^+$ CD16$^-$), intermediate (CD14$^+$ CD16$^+$), and nonclassical (CD14$^-$CD16$^{+)}$ monocytes, as well as DC subsets, when overlaid with conventional sequential gating strategy (Fig. 5 *B* and *C*). Within the monocyte clusters, we observed CD169$^+$ cells within the CD14$^+$ monocyte population that represented 5 to 15% of all CD14$^+$ monocytes (Fig. 5 *C* and *E*). After incubation of PBMCs with ganglioside-liposomes, DiD$^+$ cells were restricted to CD169-expressing cells, most notably those found in CD14$^+$ population (Fig. 5*D*). Furthermore, CD14$^+$ CD169$^+$ monocytes, but not CD14$^+$ CD169$^-$ monocytes, efficiently took up all ganglioside-liposomes, in particular those containing GD1a and GT1b (Fig. 5 *F* and *G* and *SI Appendix*, Fig. S4).

Since we observed DiD$^+$ cells in nonmonocytic clusters (Fig. 5*D*), we further assessed ganglioside-liposome targeting in DC populations by excluding CD14$^+$ and CD16$^+$ cells prior to viSNE analysis. When we overlaid manually gated DC populations onto the tSNE map, we were able to identify clusters of CD123$^+$ pDC, CD1c$^+$ cDC2, CD141$^+$ cDC1, and the recently described Axl$^+$ Siglec-6$^+$ DCs (31) (Fig. 6 *A* and *B*). The expression of CD169 was specifically restricted to Axl$^+$ DCs (Fig. 6 *A* and *C*), and these cells were present at similar frequency as CD141$^+$ cDC1 in the circulation (Fig. 6*D*). Interestingly, ganglioside-liposomes were exclusively taken up by Axl$^+$ DCs, but not other DC subsets (Fig. 6 *E*–*G* and *SI Appendix*, Fig. S4). Notably, the ganglioside-liposome uptake by the Axl$^+$ DCs was CD169-dependent (Fig. 6*G*).

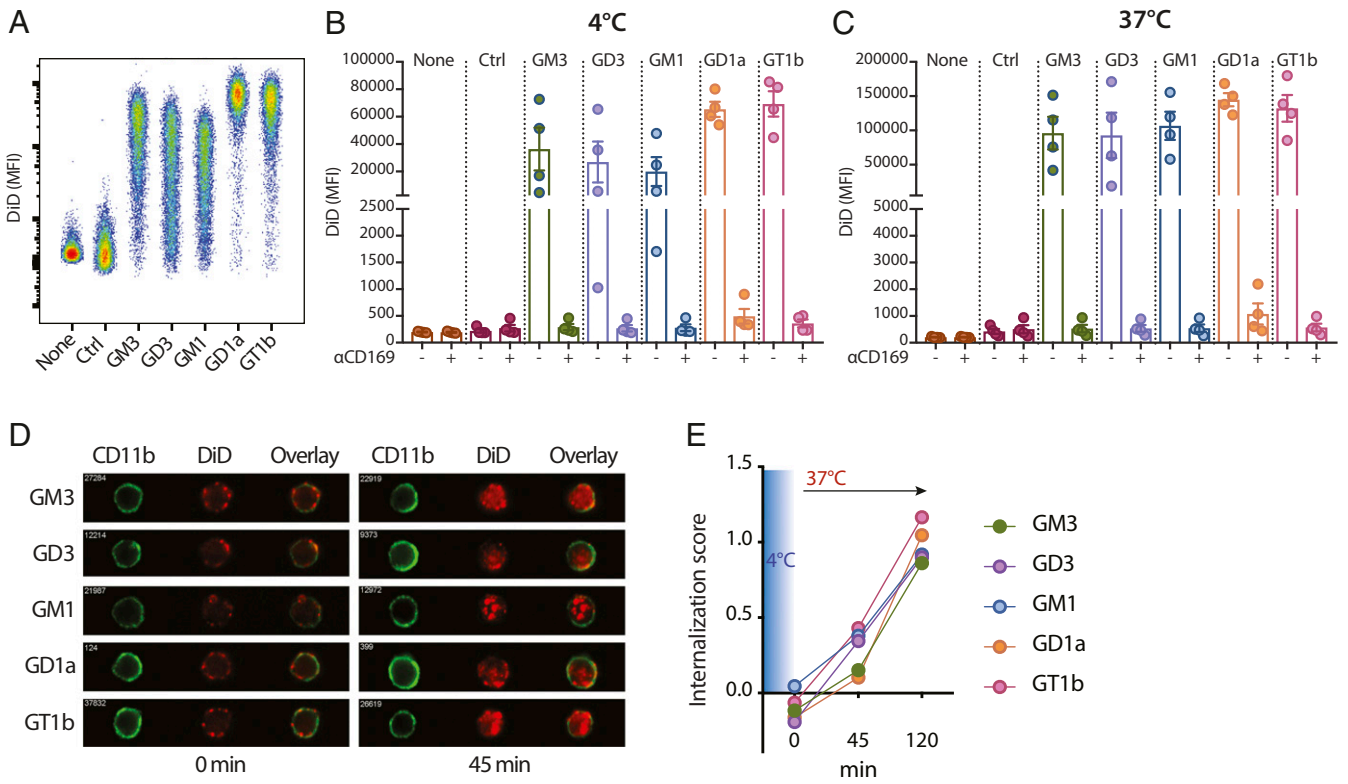

Fig. 3. Ganglioside-liposomes bind to CD169-expressing moDCs. (*A*–*C*) Ganglioside-liposomes were incubated with IFN-I–treated moDCs, and binding (4 °C; *A* and *B*) and uptake (37 °C; *C*) was determined by flow cytometry. Ctrl, control. In some conditions, moDCs were preincubated with anti-CD169 blocking antibody. Data are mean ± SEM from four donors. (*D* and *E*) After 45 min binding (4 °C), ganglioside-liposome internalization at 37 °C was measured by imaging cytometry. (*D*) Representative images and (*E*) quantification of internalization are shown. Data are representative of two independent experiments from two donors.

Moreover, no ganglioside-liposome uptake by CD169-negative lymphoid cells or granulocytes was observed (*SI Appendix*, Fig. S5).

Ganglioside-Liposomes Induce T Cell Activation by Blood-Derived Axl$^+$ DCs. To determine whether ganglioside-liposomes can deliver antigen to Axl$^+$ DCs for presentation to CD8$^+$ T cells, we enriched for total DCs from PBMCs by depleting monocytes, T cells, B cells, and NK cells and added GM3-liposomes containing WT1 tumor antigen and R848 as adjuvant (Fig. 6*H*). We selected R848 as adjuvant since Axl$^+$ DCs express TLR7 but not TLR4, and we were able to detect TNFα production by Axl$^+$ DCs treated with GM3/R848 liposome (*SI Appendix*, Fig. S6 *A* and *B*). Importantly, DCs incubated with GM3/WT1/R848 liposomes were able to stimulate IFNγ production of WT1-specific CD8$^+$ T cells that was significantly higher than the amount obtained by Ctrl/WT1/R848 liposomes (Fig. 6*I*). None of the other ganglioside-liposomes we tested were able to induce IFNγ production by WT-1–specific CD8$^+$ T cells (*SI Appendix*, Fig. S6 *C* and *D*). Additionally, GM3/R848 liposomes devoid of WT1 antigen did not induce IFNγ production (*SI Appendix*, Fig. S6*D*). Since GM3 only binds to Axl$^+$ DCs and not to other DC subsets, this indicates that GM3-liposomes specifically target and deliver antigen to circulating Axl$^+$ DCs for antigen presentation to CD8$^+$ T cells.

Axl$^+$ DCs Are Present in Cancer Patients and Can Be Targeted by Ganglioside-Liposomes. To determine the feasibility of ganglioside-liposome as nanovaccine in cancer patients, we next investigated the presence of Axl$^+$ DCs in patients with gastrointestinal malignancies, pancreatic ductal adenocarcinoma (PDAC), hepatocellular carcinoma (HCC), colorectal liver metastasis (CRLM), and melanoma. Using flow cytometry, we were able to detect Axl$^+$ DCs in all cancer patients tested (Fig. 7*A*). We also observed high expression of CD169 in Axl$^+$ DCs as compared to other DC subsets (Fig. 7*B*). Furthermore, ganglioside-liposomes were significantly taken up by Axl$^+$ DCs of these patients (Fig. 7*C*).

In conclusion, ganglioside-liposomes specifically target CD169$^+$ APCs, including Axl$^+$ DCs in cancer patients, and incorporation of adjuvant and tumor antigens can activate CD169$^+$ DCs and facilitate cross-presentation of tumor antigens to CD8$^+$ T cells.

Discussion

Liposomes have emerged as an attractive type of nanocarrier for vaccines owing to their high payloads and customizable properties (51). The addition of molecules that enable the binding to specific cell type receptors on APCs can enhance antigen uptake and subsequent T cell activation. Here, we demonstrate proof-of-concept data of a liposome-based nanovaccine carrier that targets human CD169-expressing APCs with high specificity by using gangliosides as the endogenous CD169-targeting ligands. Using an ex vivo binding/uptake approach, we demonstrate that ganglioside-liposomes bind efficiently to CD169-expressing APCs, including moDCs, CD14$^+$ CD169$^+$ monocytes, and the recently described Axl$^+$ DCs. Although other sialic acid-binding receptors such as Siglec-3, -7, and -9 and Siglec-2 and -6 are expressed by moDCs and Axl$^+$ DCs, respectively, the binding and uptake of ganglioside-liposomes was exclusively mediated by the CD169 receptor (48). Other cells lacking CD169 expression, including T cells, B cells, and NK cells, and other DC subsets, were not targeted by ganglioside-liposomes. Moreover, we demonstrate that uptake

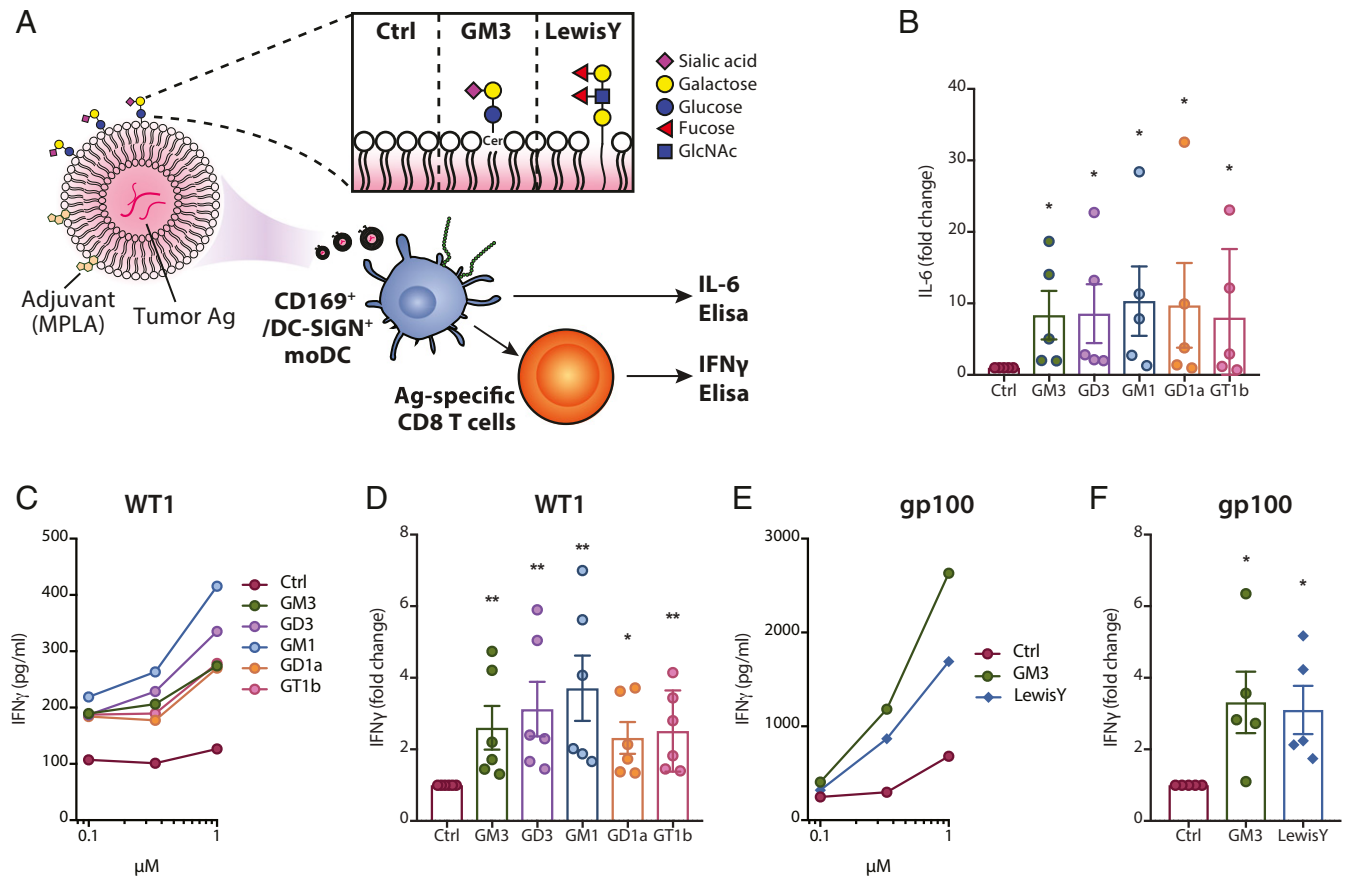

Fig. 4. Adjuvant/tumor antigen-containing ganglioside-liposomes activate CD169-expressing moDCs and are cross-presented to antigen-specific T cells. (*A*) Ganglioside- (i.e., GM3) or Lewis Y-liposomes with MPLA and/or tumor-associated antigen for moDC activation or antigen presentation assay. GlcNAc, N-acetylglucosamine. (*B*) moDCs were incubated with MPLA-containing ganglioside-liposomes at 4 °C and washed, and IL-6 secretion after 24 h was measured by ELISA. Values are calculated as fold change over control liposome; data are mean ± SEM from five donors. (*C* and *D*) Ganglioside-liposomes containing short WT1 peptide and MPLA were loaded to moDCs and washed away, and WT1-specific $CD8^+$ T cells were added. IFNγ secretion after 24 h was determined by ELISA. (*C*) Secreted IFNγ at different doses of liposomes are shown (data pooled from $n = 6$ donors). (*D*) Production of IFNγ after exposure to 1 μM ganglioside-liposomes normalized to control liposomes. Data are mean ± SEM from six donors. (*E* and *F*) GM3- or Lewis Y-liposome containing long gp100 peptide was loaded to moDCs, followed by 24 h coculture with gp100-specific T cell clone. IFNγ production by gp100-specific T cells (*E*) at different doses of liposomes (pooled from five donors) and (*F*) after treatment with 1 μM GM3- or Lewis Y-liposome normalized to control liposome. Data are mean ± SEM from five donors. Kruskal–Wallis multiple two-tailed *t* tests using a two-stage linear step-up procedure of Benjamini, Krieger, and Yekutieli, with Q = 0.05, was used (*adjusted $P < 0.05$, **adjusted $P < 0.01$).

of tumor antigen-containing ganglioside-liposomes by moDCs and Axl^+ DCs results in cross-presentation to $CD8^+$ T cells. These data together indicate that ganglioside-containing liposomes can be utilized as vaccine nanocarriers to specifically target human $CD169^+$ APCs for an effective antigen delivery and antigen-specific T cell activation (Fig. 7*D*).

While we show very specific binding of liposomes containing endogenously expressed gangliosides to CD169/Siglec-1, a recent study employed liposomes containing the synthetic glycan $3'^{BPC}$NeuAc as a vaccination strategy in mice. The $3'^{BPC}$NeuAc-liposomes were able to target mouse $CD169^+$ macrophages in vitro and in vivo, and stimulated antigen-specific T cell and NKT cell activation in mice (52, 53). The synthetic glycan $3'^{BPC}$NeuAc binds to CD169 with high affinity, whereas the endogenous ligands have much lower affinity (54). Nevertheless, our results clearly demonstrate that incorporation of the low endogenous affinity ligands in liposomes is sufficient for efficient targeting to ex vivo human APCs that express CD169 and also leads to the activation of T cell responses. One potential disadvantage of using a synthetic ligand for CD169 is the possibility of inducing a neutralizing immune response against the synthetic ligand itself. This has been shown for the addition of PEG to the surface of liposomes and is known as the accelerated blood clearance phenomenon that interferes with repeated administrations (55–57). In contrast, the use of an endogenous broadly expressed ganglioside such as GM3 would not be expected to result in antibody responses, allowing for repeated booster vaccination, and would thus be preferable to synthetic analogs.

Human CD169 is highly expressed by macrophages in the perifollicular zone of the spleen and subcapsular sinus of lymph nodes and at a lower level by splenic red pulp macrophages, which is very similar to the expression observed in mice (21, 47, 58). Higher frequencies of $CD169^+$ macrophages in tumor-draining lymph nodes have been associated with favorable prognosis in multiple cancer types (28–30). We and others have shown that antigen targeting to $CD169^+$ macrophages results in strong $CD8^+$ T cell responses in mouse in vivo models due to efficient transfer of antigens from splenic $CD169^+$ macrophages to cDC1 for $CD8^+$ T cell activation (18–21). Although still unknown, it is possible that a similar antigen transfer process between $CD169^+$ macrophages and DCs exists in humans, as has been shown between human cDC2 and cDC1 (59).

Next to macrophages, human Axl^+ DCs were recently identified in PBMCs as a separate DC subset that constitutively

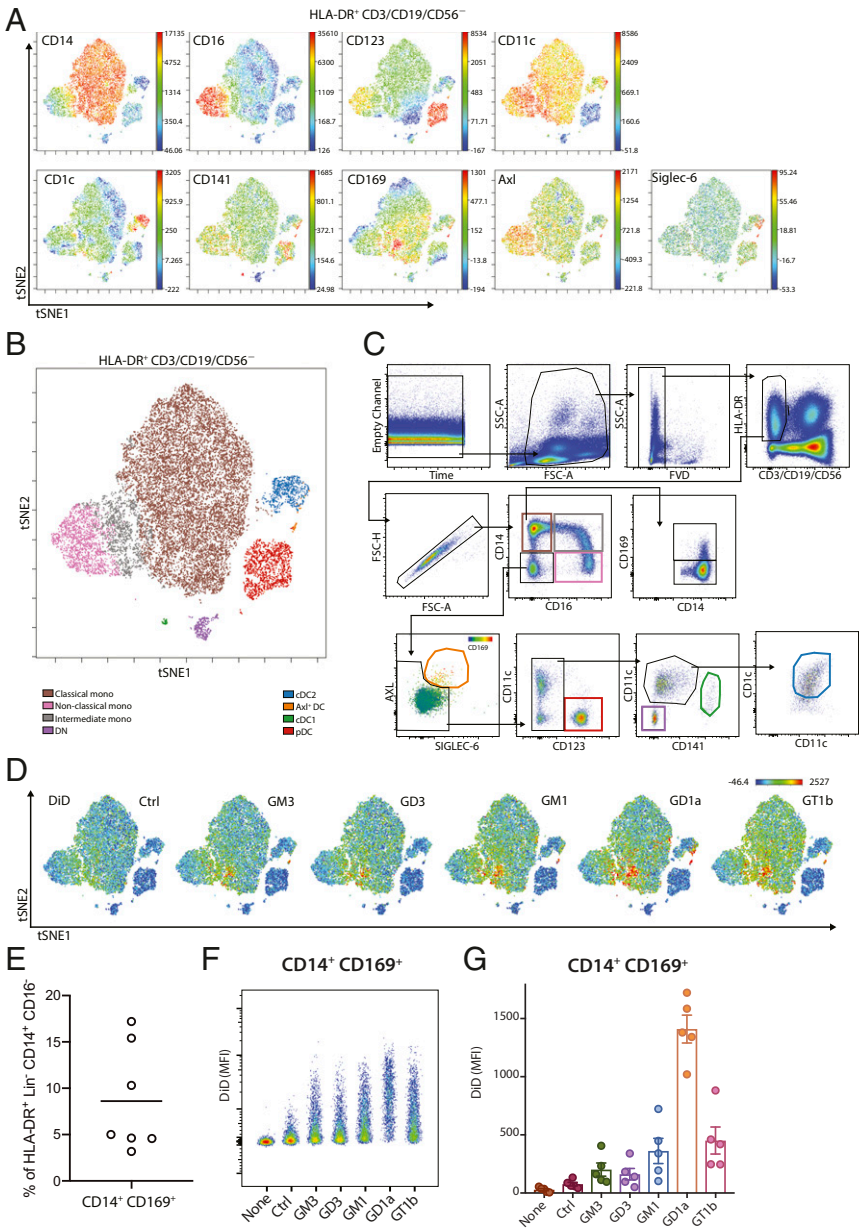

Fig. 5. Ganglioside-liposomes target human CD14$^+$ CD169$^+$ monocytes. (*A*) High-dimensionality reduction analysis of circulating HLA-DR$^+$ CD3/CD19/CD56$^-$ cells using the expression of monocytes and DC subset markers CD14, CD16, CD123, CD11c, CD1c, CD141, Axl, Siglec-6, and CD169 using viSNE analysis. (*B*) Overlay of viSNE map with (*C*) conventional gating identifies classical monocytes, nonclassical monocytes, intermediate monocytes, plasmacytoid DCs (pDC), conventional DC1 (cDC1), conventional DC2 (cDC2), and Axl$^+$ Siglec-6$^+$ DCs (Axl$^+$ DC). DN defines CD11c$^-$ CD123$^-$ cells. (*D*) Uptake of DiD-labeled ganglioside-liposomes is restricted to CD169$^+$ populations on viSNE map. Ctrl, control. (*E*) Percentage of CD14$^+$ CD169$^+$ cells within classical monocytes (HLA-DR$^+$ CD14$^+$ CD16$^-$ Lin$^-$ cells; $n = 7$). (*F* and *G*) Ganglioside-liposome uptake by human CD14$^+$ CD169$^+$ monocytes as (*F*) representative plot and (*G*) quantification ($n = 5$) is shown. Data are mean ± SEM from five donors.

expressed CD169 (31–33). These cells are present in conventional CD123$^+$ pDC preparation and show cDC-like properties. Axl$^+$ DCs also have the plasticity to differentiate into cDCs or pDCs and were shown to have potent capacity to activate CD4$^+$ and CD8$^+$ T cells in allogeneic assays. In addition, "pure" pDCs devoid of Axl$^+$ DCs have been shown to differentiate into three distinct populations with differential CD80/PD-L1 expression after microbial stimulation. One of these populations shows cDC-like features reminiscent of Axl$^+$ DCs, producing low IFNα and showing the capability of activating T cells (60). Interestingly, both the Axl$^+$ DCs as well as the pDC-derived cells express CD169 and can potentially be targeted by ganglioside-liposome. Our studies show that ganglioside-liposomes can simultaneously induce TNFα production and specifically deliver tumor antigens to Axl$^+$ DCs, which stimulate CD8$^+$ T cell responses. We also provide evidence that Axl$^+$ DCs are present and can be targeted by our nanovaccine in the circulation of patients with multiple types of cancers. These results support our hypothesis that cancer vaccines targeting human CD169$^+$ APCs are expected to boost anticancer immune responses in patients and that ganglioside-liposomes constitute an effective nanovaccine platform for tumor antigens and adjuvant.

CD169/Siglec-1 was first described as a receptor that mediates cell–cell adhesion through recognition of sialic acid-containing

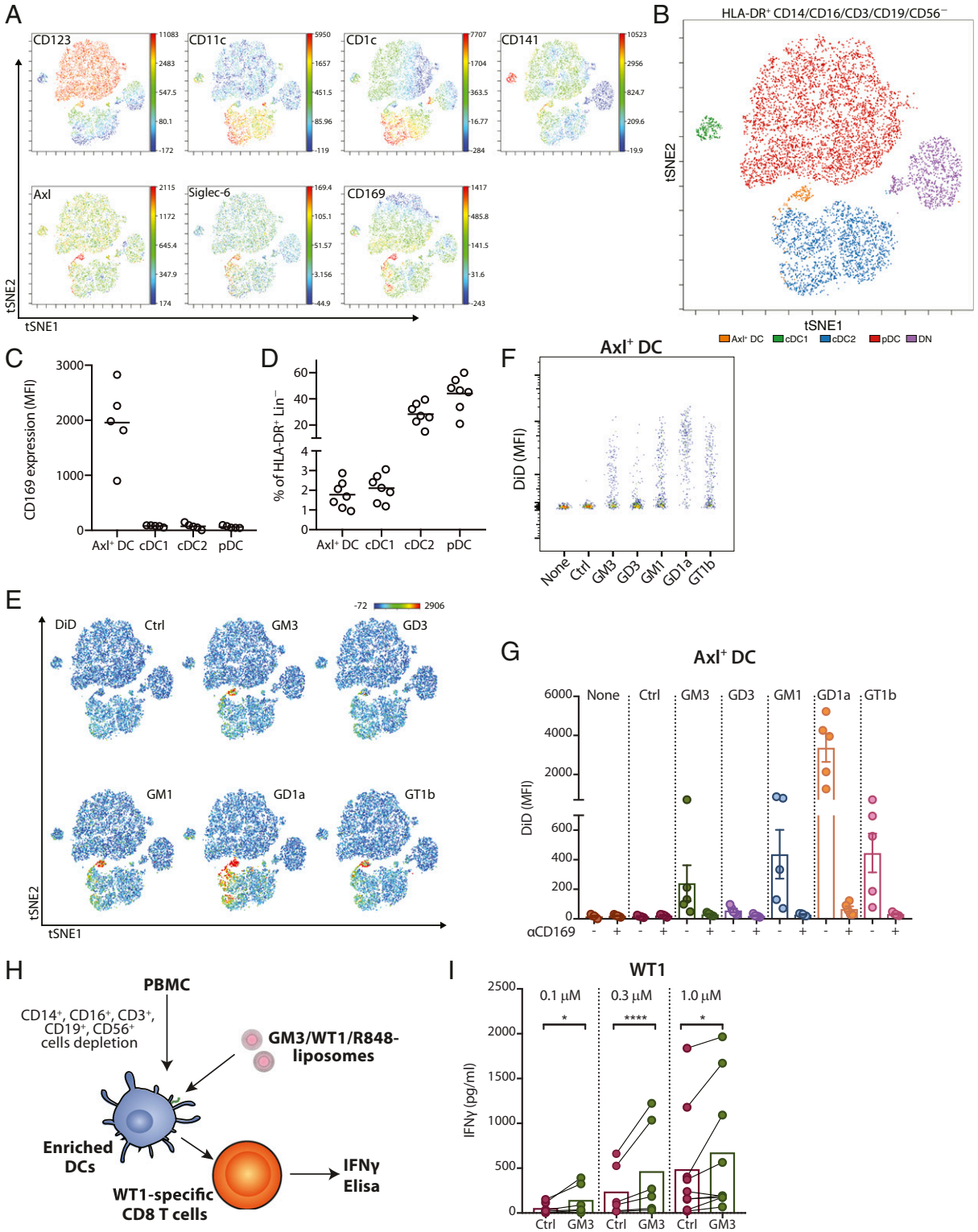

Fig. 6. Human Axl$^+$ DCs take up ganglioside-liposomes and stimulate CD8$^+$ T cells. (*A*) High-dimensionality reduction analysis of circulating HLA-DR$^+$ CD3/CD19/CD56/CD14/CD16$^-$ cells using the expression of DC subsets markers CD123, CD11c, CD1c, CD141, Axl, Siglec-6, and CD169 using viSNE analysis. (*B*) Overlay of viSNE map with conventional gating identifies plasmacytoid DCs (pDC), conventional DC1 (cDC1), conventional DC2 (cDC2), and Axl$^+$ Siglec-6$^+$ DCs (Axl$^+$ DC). DN defines CD11c$^-$CD123$^-$ cells. (*C*) The expression of CD169 on DC subsets is shown ($n = 5$). (*D*) Distribution of DC populations within HLA-DR$^+$ Lin(CD3/CD19/CD56/CD14/CD16)$^-$ cells ($n = 7$). (*E*) Uptake of DiD-labeled ganglioside-liposomes is restricted to Axl$^+$ DC population on viSNE map. (*F* and *G*) Ganglioside-liposome uptake by human Axl$^+$ DCs as (*F*) representative plot and (*G*) quantification ($n = 5$) is shown. Ctrl, control. In some conditions, cells were pre-incubated with anti-CD169 blocking antibody to block ganglioside-liposome binding. Data are mean ± SEM from $n = 4$ to 5 donors. (*H* and *I*) After lineage depletion, enriched DCs were incubated with different concentrations of GM3/WT1/R848 liposome or control liposome at 37 °C and washed, and WT1-specific CD8$^+$ T cells were added. (*I*) IFNγ secretion after 24 h was determined by ELISA. Data are means from six to nine donors (paired *t* test: $^*P < 0.05$, $^{****}P < 0.001$).

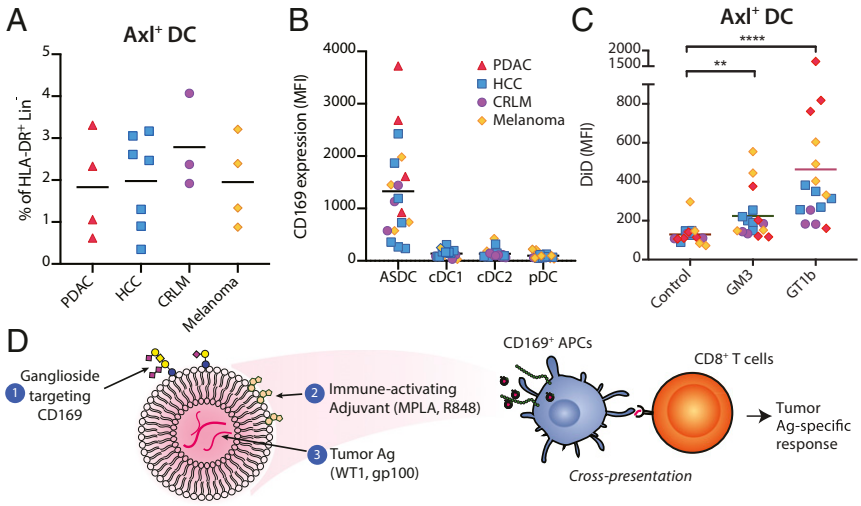

Fig. 7. Axl$^+$ DCs are present in cancer patients and can be targeted by ganglioside-liposomes. (*A*) Percentage of Axl$^+$ DCs within HLA-DR$^+$ Lin(CD3/CD19/CD56/CD14/CD16)$^-$ cells in patients with pancreatic ductal adenocarcinoma (PDAC; $n = 4$), hepatocellular carcinoma (HCC; $n = 7$), colorectal liver metastasis (CRLM; $n = 3$), and melanoma ($n = 4$). (*B*) The expression of CD169 on DC subsets of cancer patients is shown. (*C*) Ganglioside-liposome uptake by Axl$^+$ DCs of cancer patients is shown. Friedman test using a two-stage linear step-up procedure of Benjamini, Krieger, and Yekutieli, with Q = 0.05, was used (**adjusted $P <$ 0.01, ****adjusted $P < 0.0001$). (*D*) In this study, we have designed nanovaccine carriers targeting CD169$^+$ APCs, particularly Axl$^+$ DCs, using liposomes that contain (*1*) gangliosides to target CD169, (*2*) immune-activating adjuvant, and (*3*) encapsulated tumor antigen. Uptake of ganglioside-liposomes by CD169$^+$ DCs will lead to cross-presentation and activation of tumor-specific CD8$^+$ T cells.

glycolipid or glycoproteins (17, 37, 61). In the context of infection, CD169 functions as a binding receptor for sialylated bacteria, promoting phagocytosis while limiting dissemination (62). CD169 also captures viral pathogens, although it plays dual roles in host defense against viruses by triggering antiviral immune responses and permitting transinfection. By incorporating host-derived sialic acid-containing molecules on the membrane, viruses are able to bind to CD169 receptor expressed on APCs. After initial capture by CD169$^+$ macrophages or DCs, they can further transinfect other myeloid or lymphoid cells, as has been clearly demonstrated for MLV and HIV (41, 43, 45, 63). The incorporation of host-derived ganglioside GM3, in particular, has been shown to be crucial for HIV entry to human moDCs, and ganglioside-containing nanoparticles have been used as a model to study viral infection of DCs (22, 64, 65). Due to the high CD169 expression by Axl$^+$ DCs, HIV was shown to preferentially infect Axl$^+$ DC as compared to the other DC subsets (66). The ganglioside-liposomes investigated in this study mimic viral entry to CD169$^+$ APCs and specifically target human blood Axl$^+$ DCs, but not cDCs and pDCs. Since Axl$^+$ DCs express viral nucleic acid sensors such as TLR7 and TLR9, but not other TLRs, we further incorporated the TLR7 ligand R848 in the GM3-liposomes. Our data show that the combination of both components results in a virus-like nanovaccine capable to target Axl$^+$ DCs and to stimulate T cells.

In addition to CD169/Siglec-1, DC-SIGN is a well-known receptor for HIV expressed on moDCs that also functions as a target molecule for cancer vaccines (17, 67). Interestingly, many similarities exist between CD169 and DC-SIGN. Both molecules are expressed by perifollicular macrophages in the human spleen and by IFN-I–treated moDCs (21, 58, 68). They function as a receptor for a variety of pathogens, but are also adhesion molecules for immune cells and can mediate transinfection of viruses (67, 69). As such, human CD169$^+$ DC-SIGN$^+$ perifollicular macrophages function similarly as mouse CD169$^+$ metallophilic marginal-zone macrophages, that is, they both capture and transfer antigen to other immune cells, such as DCs and B cells, to initiate antigen-specific adaptive immune responses (22). This is crucial in the context of vaccine delivery and T cell activation for cancer immunotherapy. Indeed, we and others have previously shown that antigen targeting toward DC-SIGN using antibodies induces efficient antigen-specific T cell responses in in vitro and in vivo models (15, 70, 71). Using fucose-containing glycans as ligands to target DC-SIGN, we previously generated liposome or dendrimers to codeliver antigen and adjuvant to DC-SIGN$^+$ DCs. These nanoparticles could efficiently target moDCs for activation of antigen-specific T cells (50, 72, 73). In this paper, we show that ganglioside-liposomal antigen targeting to CD169 on moDCs results in a comparable T cell activation as that observed by antigen targeting toward DC-SIGN using Lewis Y-liposome. Additionally, we have previously demonstrated that antibody-mediated tumor antigen targeting to CD169 and DC-SIGN provided comparable T cell activation by moDCs (21). However, DC-SIGN is not expressed by circulating DCs, whereas CD169 is expressed by Axl$^+$ DCs, thus underlining the potential advantage of CD169 targeting.

Finally, the optimal route of administration of DC targeting using nanoparticles is dependent on their formulation (74). Recent studies indicate that i.v. delivery of vaccines for malaria and *Mycobacterium tuberculosis* is superior to peripheral delivery (75–77), and this route has also been utilized for cancer vaccines that consist of RNA- or DNA-lipoplexes (78–80). Importantly, i.v. systemic delivery of liposomal-based vaccines was shown to be more potent in inducing strong antitumor T cell responses than the peripheral injection routes (78, 80). Hence, we predict that i.v. delivery of vaccines that target antigen to CD169 will enable uptake by perifollicular macrophages in the spleen and Axl$^+$ DCs in the circulation, leading to an efficient antitumor CD8$^+$ T cell induction.

Taken together, our study reveals proof-of-concept data for ganglioside-liposomes as nanovaccine carriers targeting human CD169$^+$ APCs in a highly specific manner. Targeting CD169$^+$ APCs using nanoparticles is expected to function as an effective antigen delivery platform to drive CD8$^+$ T cell responses. Future research assessing different type of TLR ligands and tumor (neo-)epitopes, in combination with checkpoint inhibition, will further optimize this vaccination strategy.

Materials and Methods

Human Primary Cells and Patients. Human peripheral blood mononuclear cells (PBMCs) from heparinized blood were isolated by density gradient centrifugation (Lymphoprep; Axis-Shield). PBMCs were collected from patients with gastrointestinal malignancies or metastatic melanoma in accordance with the Helsinki Declaration of 1975 and with approval by the institutional review board of the Amsterdam UMC. All subjects provided informed consent. Samples were deidentified prior to use in the study. PDAC, HCC, and CRLM patients were enrolled in the HPB biobank at the VU University Medical Center (Medical Ethical Committee approval 2016.510). Melanoma patients were enrolled in a clinical study of autologous whole-cell vaccination at the VU University Medical Center between 1987 and 1998 (81). Leftover human spleen tissue was obtained anonymously from the VUmc Biobank (BUP 2015–074); therefore, approval by the medical ethical committee was not required. Human spleen was mechanically and enzymatically digested with Liberase and DNase I (Roche) at 37 °C for 30 min. Cells were then depleted of red blood cells using ammonium chloride lysing buffer. Following PBS washes, cells were further processed for liposome binding or uptake or flow cytometry staining as described below.

Monocyte-Derived DCs and Macrophages and Primary DC Preparation. Monocytes isolated using Percoll gradient or CD14-magnetic beads (Miltenyi Biotec) were cultured for 5 to 6 d in RPMI 1640 complete medium (Thermo Fisher Scientific) containing 10% fetal calf serum (Biowest), 50 U/mL penicillin, 50 μg/mL streptomycin, and 2 mM glutamine (all from Thermo Fisher Scientific). For generation of moDCs, monocytes were cultured in the presence of recombinant human IL-4 (500 U/mL) and GM-CSF (800 U/mL; both from Immunotools). For generation of moMacs, recombinant human M-CSF (50 ng/mL; Miltenyi Biotec) was used. To increase CD169 expression, cells were treated with recombinant human IFNα (1,000 U/mL; Miltenyi Biotec) during the last 2 d of culture. For enrichment of primary DCs, PBMCs were depleted from non-DC populations using biotinylated antibodies against CD3, CD14, CD19, CD56 (10 μg/mL; all produced and validated in-house), and CD16 (5 μg/mL; Biolegend) and streptavidin nanobeads (Biolegend) using an LD Column (Miltenyi).

Cell Lines. THP-1 cells overexpressing CD169/Sialoadhesin/Sn (TSn) were maintained in RPMI complete medium (35). $WT1_{126–134}$ or $gp100_{280–288}$ retroviral TCRαβ-transduced HLA-A2.1 restricted T cell lines were maintained in Yssel's medium: IMDM (Thermo Fisher Scientific), 20 μg/mL human transferrin (Boehringer Ingelheim), 2 μg/mL linoleic acid, 2 μg/mL palmitic acid (all from Calbiochem), 5 μg/mL insulin, 0.25% BSA, 1.8 μg/mL 20-amino ethanol, 1% human serum (all from Sigma-Aldrich), penicillin, streptomycin, glutamine, and IL-2 (100 IU/mL; Peprotech) as previously described (73, 82, 83).

Liposome Preparation. Liposomes were prepared from a mixture of phospholipids and cholesterol utilizing the film extrusion method as described previously and depicted in *SI Appendix*, Fig. S1 (49, 72). In brief, egg phosphatidylcholine (EPC)-35 (Lipoid), egg phosphatidylglycerol (EPG)-Na (Lipoid), and cholesterol (Sigma-Aldrich) were mixed at a molar ratio of 3.8:1:2.5. Ganglioside (3 mol%; GM3, GD3, GM1; Avanti Polar Lipids; GD1a, GT1b; Matreya) and 0.1 mol% of lipophilic fluorescent tracer DiD (1,1′-dioctadecyl-3,3,3′,3′-tetramethylindodicarbocyanine; Thermo Fisher Scientific) were added to the mixture. Where specified, TLR-ligand MPLA (2 mol%; Invivogen) or R848 (4 mol%; Invivogen) was included. The solvent was evaporated under vacuum on a rotavapor to generate a lipid film, and the residual organic solvent was removed by nitrogen flush. The lipid film was then hydrated in Hepes-buffered saline (10 mM Hepes buffer, pH 7.4, 0.8% NaCl) with mechanical agitation by hand-shaking or rotary mixing for 20 min until the lipid film was completely resuspended. For antigen-presentation assay, the pancreatic cancer-associated antigen Wilms' Tumor 1 short peptide (RMFPNAPYL) and melanoma-associated antigen gp100 long peptide (VTHTYLEPGPVTANRQLYPEWTEAQRLD; both 3 mg/mL) were encapsulated into the liposomes during the hydration step. Peptides were produced by solid-phase peptide synthesis using Fmoc-chemistry with a Symphony peptide synthesizer (Protein Technologies). The liposomes were sized by sequential extrusion through two stacked polycarbonate filters (400 and 200 nm) with a Lipex high-pressure extrusion device (Northern Lipids). Nonincorporated materials were removed by sedimentation of the liposomes by ultracentrifugation at 200,000 × *g* twice. The final resuspension of the liposomes was performed in Hepes buffer at pH 7.4. The mean particle size, polydispersity index, and zeta potential were measured using Malvern Zetasizer (Malvern Instruments). Phospholipid concentrations were determined by a colorimetric phosphate assay. Briefly, liposome dispersions were dried in glass test tubes for 30 min at 180 °C and degraded by the addition of 0.3 mL 70% perchloric acid, followed by another 30-min incubation at 180 °C. After cooling, 1 mL of water, 0.5 mL of 1.2% hexa-ammoniummolybdate solution, and 0.5 mL of 5% (wt/vol) ascorbic acid were added, mixed, and heated in boiling water for 5 min. Absorbance values were measured at 797 nm against a calibration curve prepared with sodium phosphate (NaH_2PO_4). Physical properties of liposomes are shown in *SI Appendix*, Table S1.

Recombinant CD169 ELISA. Liposomes (25 nM) were coated and fixed in 100% ethanol on a Nunc MaxiSorp ELISA plate (Thermo Fisher Scientific) and air-dried overnight. This was followed by blocking with 1% BSA (BSA, fraction V, fatty acid-free; Calbiochem)/phosphate-buffered saline (PBS), washes with PBS, and incubation with 1 μg/mL recombinant human CD169 with C-terminal 6-His tag (R&D Systems) for 1 h at RT. For detection, incubation with HRP-conjugated anti-His (Biolegend) in 1% BSA/PBS for 30 min at RT was performed, followed by PBS washes and the addition of TMB as substrate (Sigma-Aldrich). Absorbance was measured at 450 nm using a microplate spectrophotometer (Bio-Rad).

Cell-Based Liposome Binding and Uptake. Cells were incubated with ganglioside-liposomes (100 nM unless indicated otherwise) for 45 min at 4 °C or 37 °C to evaluate liposome binding or uptake, respectively. Specific binding or uptake of ganglioside-liposomes mediated by CD169 was determined by preincubation of cells for at least 15 min at 4 °C with 2 μg/mL neutralizing antibody against CD169, clone 7–239.

Flow Cytometry. Cells were incubated with Fc block (BD Biosciences, cat. no. 564219) and viability dye (fixable viability dye eFluor 780, FVD; eBioscience) prior to cell surface staining with fluorescence-conjugated antibodies in 0.5% BSA/PBS for 20 min at 4 °C. After thorough washes, cells were fixed with 2% paraformaldehyde for 10 min at RT. For intracellular staining, cells were additionally incubated with antibodies in 0.5% BSA/PBS with 0.5% saponin for 20 min at 4 °C. Cells were acquired on a Fortessa (BD Biosciences) or Aurora spectral flow cytometer (Cytek) and analyzed with FlowJo software (Tree Star). High-dimensionality reduction analysis viSNE was performed using Cytobank software. Antibodies clones and dilutions used are listed in *SI Appendix*, Table S2.

Imaging Cytometry. To investigate liposome uptake, moDCs were incubated with liposomes for 45 min at 4 °C, washed, and placed at 37 °C for the indicated time points. moDCs were stained for cell surface CD11b for 20 min at 4 °C, washed, and fixed as mentioned above. Cells were acquired at Amnis Imagestream instrument and analyzed by Amnis IDEAS software.

DC Activation and Antigen Presentation. IFNα-treated HLA-$A2^+$ moDCs were seeded at a concentration of 2×10^4 cells per well in U-bottom 96-well plates. MPLA-incorporated ganglioside-liposomes were added to moDCs (45 min, 4 °C), and IL-6 secretion by DCs in the supernatant was measured after 24 h using ELISA (Thermo Fisher Scientific). For Axl^+ DC cytokine measurement, PBMCs were incubated with ganglioside-liposomes at 37 °C for 45 min, washed, and cultured for 4 h in RPMI complete medium, with the addition of Brefeldin A (BD GolgiPlug) for the final 3 h. TNFα production was measured by intracellular flow cytometry. For antigen presentation, moDCs or enriched DCs were incubated with ganglioside-liposomes encapsulating WT1 short peptide (45 min, 4 °C for moDCs, 37 °C for enriched DCs) or gp100 long peptide (3 h, 37 °C), followed by medium washes. LPS (100 ng/mL; Sigma-Aldrich) was added for gp100 presentation. Antigen-loaded DCs were then cocultured overnight with $WT1_{126–134}$ or $gp100_{280–288}$ TCR-transduced HLA-A2.1 restricted T cell lines (4 to 5 × 10^4 cells per well) at a ratio of moDC:T cells of 1:5 or enriched DC:T cells of 1:1. After 24 h, production of IFNγ in the supernatants of the cocultures was determined by ELISA (eBioscience).

Statistics. Statistical analysis of Kruskal–Wallis multiple two-tailed *t* tests; Friedman test corrected using a two-stage linear step-up procedure of Benjamini, Krieger, and Yekutieli; or paired *t* test were performed using GraphPad Prism 8 (GraphPad Software).

Data Availability. All study data are included in the article and supporting information.

ACKNOWLEDGMENTS. This work was supported by grants from the Dutch Cancer Society (VU2016-10449) to J.M.M.d.H., Y.v.K., and T.D.d.G.; from the Phospholipid Research Center to J.M.M.d.H. and Y.v.K.; from NWO ZonMW (TOP 91218024) to J.M.M.d.H. and G.S.; and by an EU Research Framework

Program Grant (H2020-MSCA-ITN-2014-ETN-642870) to DC4U/M.L.V. We thank Sven Bruijns, Larissa Klaase (Amsterdam UMC), and Louis van Bloois (Utrecht University) for their technical advice and expertise. We acknowledge Jan Verhoeff, Dr. Juan Garcia Vallejo, and the Microscopy and Cytometry Core Facility at the Amsterdam UMC–Location VUmc for providing assistance in microscopy and cytometry. We thank Daan J. Brinkman (Amsterdam UMC, Catharina Hospital) and Wouter J. de Jonge (Amsterdam UMC) for additional patient material.

1. A. Haslam, V. Prasad, Estimation of the percentage of US patients with cancer who are eligible for and respond to checkpoint inhibitor immunotherapy drugs. *JAMA Netw. Open* **2**, e192535 (2019).
2. M. Yarchoan, A. Hopkins, E. M. Jaffee, Tumor mutational burden and response rate to PD-1 inhibition. *N. Engl. J. Med.* **377**, 2500–2501 (2017).
3. C. Nevala-Plagemann, M. Hidalgo, I. Garrido-Laguna, From state-of-the-art treatments to novel therapies for advanced-stage pancreatic cancer. *Nat. Rev. Clin. Oncol.* (2019).
4. A. A. Wu, E. Jaffee, V. Lee, Current status of immunotherapies for treating pancreatic cancer. *Curr. Oncol. Rep.* **21**, 60 (2019).
5. R. H. Vonderheide, The immune revolution: A case for priming, not checkpoint. *Cancer Cell* **33**, 563–569 (2018).
6. L. Danilova *et al*., Programmed cell death ligand-1 (PD-L1) and CD8 expression profiling identify an immunologic subtype of pancreatic ductal adenocarcinomas with favorable survival. *Cancer Immunol. Res.* **7**, 886–895 (2019).
7. V. P. Balachandran *et al*.; Australian Pancreatic Cancer Genome Initiative; Garvan Institute of Medical Research; Prince of Wales Hospital; Royal North Shore Hospital; University of Glasgow; St Vincent's Hospital; QIMR Berghofer Medical Research Institute; University of Melbourne, Centre for Cancer Research; University of Queensland, Institute for Molecular Bioscience; Bankstown Hospital; Liverpool Hospital; Royal Prince Alfred Hospital, Chris O'Brien Lifehouse; Westmead Hospital; Fremantle Hospital; St John of God Healthcare; Royal Adelaide Hospital; Flinders Medical Centre; Envoi Pathology; Princess Alexandria Hospital; Austin Hospital; Johns Hopkins Medical Institutes; ARC-Net Centre for Applied Research on Cancer, Identification of unique neoantigen qualities in long-term survivors of pancreatic cancer. *Nature* **551**, 512–516 (2017).
8. Y. Ino *et al*., Immune cell infiltration as an indicator of the immune microenvironment of pancreatic cancer. *Br. J. Cancer* **108**, 914–923 (2013).
9. S. Anguille, E. L. Smits, E. Lion, V. F. van Tendeloo, Z. N. Berneman, Clinical use of dendritic cells for cancer therapy. *Lancet Oncol.* **15**, e257–e267 (2014).
10. A. Huber, F. Dammeijer, J. G. J. V. Aerts, H. Vroman, Current state of dendritic cell-based immunotherapy: Opportunities for *in vitro* antigen loading of different DC subsets? *Front. Immunol.* **9**, 2804 (2018).
11. K. F. Bol, G. Schreibelt, W. R. Gerritsen, I. J. de Vries, C. G. Figdor, Dendritic cell-based immunotherapy: State of the art and beyond. *Clin. Cancer Res.* **22**, 1897–1906 (2016).
12. M. Guilliams *et al*., Unsupervised high-dimensional analysis aligns dendritic cells across tissues and species. *Immunity* **45**, 669–684 (2016).
13. M. Collin, V. Bigley, Human dendritic cell subsets: An update. *Immunology* **154**, 3–20 (2018).
14. M. V. Dhodapkar *et al*., Induction of antigen-specific immunity with a vaccine targeting NY-ESO-1 to the dendritic cell receptor DEC-205. *Sci. Transl. Med.* **6**, 232ra51 (2014).
15. S. T. T. Schetters *et al*., Mouse DC-SIGN/CD209a as target for antigen delivery and adaptive immunity. *Front. Immunol.* **9**, 990 (2018).
16. K. M. Tullett *et al*., Targeting CLEC9A delivers antigen to human CD141$^+$ DC for CD4$^+$ and CD8$^+$T cell recognition. *JCI Insight* **1**, e87102 (2016).
17. D. van Dinther *et al*., Targeting C-type lectin receptors: A high-carbohydrate diet for dendritic cells to improve cancer vaccines. *J. Leukoc. Biol.* **102**, 1017–1034 (2017).
18. D. van Dinther *et al*., Functional CD169 on macrophages mediates interaction with dendritic cells for CD8$^+$ T cell cross-priming. *Cell Rep.* **22**, 1484–1495 (2018).
19. R. Backer *et al*., Effective collaboration between marginal metallophilic macrophages and CD8+ dendritic cells in the generation of cytotoxic T cells. *Proc. Natl. Acad. Sci. U.S.A.* **107**, 216–221 (2010).
20. D. van Dinther *et al*., Comparison of protein and peptide targeting for the development of a CD169-based vaccination strategy against melanoma. *Front. Immunol.* **9**, 1997 (2018).
21. D. van Dinther *et al*., Activation of CD8$^+$ T cell responses after melanoma antigen targeting to CD169$^+$ antigen presenting cells in mice and humans. *Cancers (Basel)* **11**, E183 (2019).
22. J. Grabowska, M. A. Lopez-Venegas, A. J. Affandi, J. M. M. den Haan, CD169$^+$ macrophages capture and dendritic cells instruct: The interplay of the gatekeeper and the general of the immune system. *Front. Immunol.* **9**, 2472 (2018).
23. D. A. P. Louie, S. Liao, Lymph node subcapsular sinus macrophages as the frontline of lymphatic immune defense. *Front. Immunol.* **10**, 347 (2019).
24. C. A. Bernhard, C. Ried, S. Kochanek, T. Brocker, CD169+ macrophages are sufficient for priming of CTLs with specificities left out by cross-priming dendritic cells. *Proc. Natl. Acad. Sci. U.S.A.* **112**, 5461–5466 (2015).
25. P. D. Uchil *et al*., A protective role for the lectin CD169/Siglec-1 against a pathogenic murine retrovirus. *Cell Host Microbe* **25**, 87–100.e10 (2019).
26. F. Pucci *et al*., SCS macrophages suppress melanoma by restricting tumor-derived vesicle-B cell interactions. *Science* **352**, 242–246 (2016).
27. L. V. Black *et al*., The CD169 sialoadhesin molecule mediates cytotoxic T-cell responses to tumour apoptotic vesicles. *Immunol. Cell Biol.* **94**, 430–438 (2016).
28. K. Ohnishi *et al*., CD169-positive macrophages in regional lymph nodes are associated with a favorable prognosis in patients with colorectal carcinoma. *Cancer Sci.* **104**, 1237–1244 (2013).
29. Y. Saito *et al*., Prognostic significance of CD169+ lymph node sinus macrophages in patients with malignant melanoma. *Cancer Immunol. Res.* **3**, 1356–1363 (2015).
30. T. Asano *et al*., CD169-positive sinus macrophages in the lymph nodes determine bladder cancer prognosis. *Cancer Sci.* **109**, 1723–1730 (2018).
31. A. C. Villani *et al*., Single-cell RNA-seq reveals new types of human blood dendritic cells, monocytes, and progenitors. *Science* **356**, eaah4573 (2017).
32. P. See *et al*., Mapping the human DC lineage through the integration of high-dimensional techniques. *Science* **356**, eaag3009 (2017).
33. M. Alcantara-Hernandez *et al*., High-dimensional phenotypic mapping of human dendritic cells reveals interindividual variation and tissue specialization. *Immunity* **47**, 1037–1050.e6 (2017).
34. R. Leylek *et al*., Integrated cross-species analysis identifies a conserved transitional dendritic cell population. *Cell Rep.* **29**, 3736–3750.e8 (2019).
35. H. Rempel, C. Calosing, B. Sun, L. Pulliam, Sialoadhesin expressed on IFN-induced monocytes binds HIV-1 and enhances infectivity. *PLoS One* **3**, e1967 (2008).
36. M. R. York *et al*., A macrophage marker, Siglec-1, is increased on circulating monocytes in patients with systemic sclerosis and induced by type I interferons and toll-like receptor agonists. *Arthritis Rheum.* **56**, 1010–1020 (2007).
37. M. S. Macauley, P. R. Crocker, J. C. Paulson, Siglec-mediated regulation of immune cell function in disease. *Nat. Rev. Immunol.* **14**, 653–666 (2014).
38. P. R. Crocker *et al*., Purification and properties of sialoadhesin, a sialic acid-binding receptor of murine tissue macrophages. *EMBO J.* **10**, 1661–1669 (1991).
39. B. E. Collins *et al*., Binding specificities of the sialoadhesin family of I-type lectins. Sialic acid linkage and substructure requirements for binding of myelin-associated glycoprotein, Schwann cell myelin protein, and sialoadhesin. *J. Biol. Chem.* **272**, 16889–16895 (1997).
40. W. B. Puryear, X. Yu, N. P. Ramirez, B. M. Reinhard, S. Gummuluru, HIV-1 incorporation of host-cell-derived glycosphingolipid GM3 allows for capture by mature dendritic cells. *Proc. Natl. Acad. Sci. U.S.A.* **109**, 7475–7480 (2012).
41. X. Sewald *et al*., Retroviruses use CD169-mediated trans-infection of permissive lymphocytes to establish infection. *Science* **350**, 563–567 (2015).
42. D. Perez-Zsolt *et al*., Anti-Siglec-1 antibodies block Ebola viral uptake and decrease cytoplasmic viral entry. *Nat. Microbiol.* **4**, 1558–1570 (2019).
43. E. Erikson *et al*., Mouse siglec-1 mediates trans-infection of surface-bound murine leukemia virus in a sialic acid N-acyl side chain-dependent manner. *J. Biol. Chem.* **290**, 27345–27359 (2015).
44. H. Akiyama *et al*., Virus particle release from glycosphingolipid-enriched microdomains is essential for dendritic cell-mediated capture and transfer of HIV-1 and henipavirus. *J. Virol.* **88**, 8813–8825 (2014).
45. N. Izquierdo-Useros *et al*., Siglec-1 is a novel dendritic cell receptor that mediates HIV-1 trans-infection through recognition of viral membrane gangliosides. *PLoS Biol.* **10**, e1001448 (2012).
46. Y. Hashimoto, M. Suzuki, P. R. Crocker, A. Suzuki, A streptavidin-based neoglycoprotein carrying more than 140 GT1b oligosaccharides: Quantitative estimation of the binding specificity of murine sialoadhesin expressed on CHO cells. *J. Biochem.* **123**, 468–478 (1998).
47. S. Q. Nagelkerke *et al*., Red pulp macrophages in the human spleen are a distinct cell population with a unique expression of Fc-γ receptors. *Blood Adv.* **2**, 941–953 (2018).
48. J. Lübbers, E. Rodríguez, Y. van Kooyk, Modulation of immune tolerance via siglec-sialic acid interactions. *Front. Immunol.* **9**, 2807 (2018).
49. M. A. Boks *et al*., MPLA incorporation into DC-targeting glycoliposomes favours anti-tumour T cell responses. *J. Control. Release* **216**, 37–46 (2015).
50. C. M. Fehres *et al*., Cross-presentation through langerin and DC-SIGN targeting requires different formulations of glycan-modified antigens. *J. Control. Release* **203**, 67–76 (2015).
51. B. S. Pattni, V. V. Chupin, V. P. Torchilin, New developments in liposomal drug delivery. *Chem. Rev.* **115**, 10938–10966 (2015).
52. W. C. Chen *et al*., Antigen delivery to macrophages using liposomal nanoparticles targeting sialoadhesin/CD169. *PLoS One* **7**, e39039 (2012).
53. N. Kawasaki *et al*., Targeted delivery of lipid antigen to macrophages via the CD169/sialoadhesin endocytic pathway induces robust invariant natural killer T cell activation. *Proc. Natl. Acad. Sci. U.S.A.* **110**, 7826–7831 (2013).
54. C. M. Nycholat, C. Rademacher, N. Kawasaki, J. C. Paulson, In silico-aided design of a glycan ligand of sialoadhesin for in vivo targeting of macrophages. *J. Am. Chem. Soc.* **134**, 15696–15699 (2012).
55. E. T. Dams *et al*., Accelerated blood clearance and altered biodistribution of repeated injections of sterically stabilized liposomes. *J. Pharmacol. Exp. Ther.* **292**, 1071–1079 (2000).
56. M. Mohamed *et al*., PEGylated liposomes: Immunological responses. *Sci. Technol. Adv. Mater.* **20**, 710–724 (2019).
57. P. Laverman *et al*., Factors affecting the accelerated blood clearance of polyethylene glycol-liposomes upon repeated injection. *J. Pharmacol. Exp. Ther.* **298**, 607–612 (2001).
58. B. Steiniger, P. Barth, B. Herbst, A. Hartnell, P. R. Crocker, The species-specific structure of microanatomical compartments in the human spleen: Strongly sialoadhesin-positive macrophages occur in the perifollicular zone, but not in the marginal zone. *Immunology* **92**, 307–316 (1997).
59. A. Silvin *et al*., Constitutive resistance to viral infection in human CD141$^+$ dendritic cells. *Sci. Immunol.* **2**, eaai8071 (2017).

60. S. G. Alculumbre *et al*., Diversification of human plasmacytoid predendritic cells in response to a single stimulus. *Nat. Immunol.* **19**, 63–75 (2018).
61. Y. Zhang *et al*., Migratory and adhesive cues controlling innate-like lymphocyte surveillance of the pathogen-exposed surface of the lymph node. *eLife* **5**, e18156 (2016).
62. M. Klaas, P. R. Crocker, Sialoadhesin in recognition of self and non-self. *Semin. Immunopathol.* **34**, 353–364 (2012).
63. W. B. Puryear *et al*., Interferon-inducible mechanism of dendritic cell-mediated HIV-1 dissemination is dependent on Siglec-1/CD169. *PLoS Pathog.* **9**, e1003291 (2013).
64. X. Yu *et al*., Glycosphingolipid-functionalized nanoparticles recapitulate CD169-dependent HIV-1 uptake and trafficking in dendritic cells. *Nat. Commun.* **5**, 4136 (2014).
65. F. Xu *et al*., Membrane-wrapped nanoparticles probe divergent roles of GM3 and phosphatidylserine in lipid-mediated viral entry pathways. *Proc. Natl. Acad. Sci. U.S.A.* **115**, E9041–E9050 (2018).
66. N. Ruffin *et al*., Constitutive Siglec-1 expression confers susceptibility to HIV-1 infection of human dendritic cell precursors. *Proc. Natl. Acad. Sci. U.S.A.* **116**, 21685–21693 (2019).
67. T. B. Geijtenbeek *et al*., DC-SIGN, a dendritic cell-specific HIV-1-binding protein that enhances trans-infection of T cells. *Cell* **100**, 587–597 (2000).
68. M. Pack *et al*., DEC-205/CD205+ dendritic cells are abundant in the white pulp of the human spleen, including the border region between the red and white pulp. *Immunology* **123**, 438–446 (2008).
69. D. Perez-Zsolt, J. Martinez-Picado, N. Izquierdo-Useros, When dendritic cells go viral: The role of siglec-1 in host defense and dissemination of enveloped viruses. *Viruses* **12**, E8 (2019).
70. P. J. Tacken *et al*., Targeting DC-SIGN via its neck region leads to prolonged antigen residence in early endosomes, delayed lysosomal degradation, and cross-presentation. *Blood* **118**, 4111–4119 (2011).
71. S. K. Horrevorts *et al*., Toll-like receptor 4 triggering promotes cytosolic routing of DC-SIGN-targeted antigens for presentation on MHC class I. *Front. Immunol.* **9**, 1231 (2018).
72. W. W. Unger *et al*., Glycan-modified liposomes boost CD4+ and CD8+ T-cell responses by targeting DC-SIGN on dendritic cells. *J. Control. Release* **160**, 88–95 (2012).
73. S. Duinkerken *et al*., Glyco-dendrimers as intradermal anti-tumor vaccine targeting multiple skin DC subsets. *Theranostics* **9**, 5797–5809 (2019).
74. S. Mitragotri, P. A. Burke, R. Langer, Overcoming the challenges in administering biopharmaceuticals: Formulation and delivery strategies. *Nat. Rev. Drug Discov.* **13**, 655–672 (2014).
75. R. Parmar *et al*., Route of administration of attenuated sporozoites is instrumental in rendering immunity against Plasmodia infection. *Vaccine* **34**, 3229–3234 (2016).
76. B. Mordmüller *et al*., Sterile protection against human malaria by chemoattenuated PfSPZ vaccine. *Nature* **542**, 445–449 (2017).
77. P. A. Darrah *et al*., Prevention of tuberculosis in macaques after intravenous BCG immunization. *Nature* **577**, 95–102 (2020).
78. L. M. Kranz *et al*., Systemic RNA delivery to dendritic cells exploits antiviral defence for cancer immunotherapy. *Nature* **534**, 396–401 (2016).
79. K. Van der Jeught *et al*., Dendritic cell targeting mRNA lipopolyplexes combine strong antitumor T-cell immunity with improved inflammatory safety. *ACS Nano* **12**, 9815–9829 (2018).
80. L. U'Ren, R. Kedl, S. Dow, Vaccination with liposome–DNA complexes elicits enhanced antitumor immunity. *Cancer Gene Ther.* **13**, 1033–1044 (2006).
81. A. Baars *et al*., Skin tests predict survival after autologous tumor cell vaccination in metastatic melanoma: Experience in 81 patients. *Ann. Oncol.* **11**, 965–970 (2000).
82. N. Schaft *et al*., Peptide fine specificity of anti-glycoprotein 100 CTL is preserved following transfer of engineered TCR alpha beta genes into primary human T lymphocytes. *J. Immunol.* **170**, 2186–2194 (2003).
83. J. Kuball *et al*., Facilitating matched pairing and expression of TCR chains introduced into human T cells. *Blood* **109**, 2331–2338 (2007).